Magnetic domain studies of $La_{0.7}Sr_{0.3}MnO_3$ film deposited on $SrLaAlO_3$ (001) substrate

2013 J. Phys. D: Appl. Phys. 46 255001

(http://iopscience.iop.org/0022-3727/46/25/255001)

J. Phys. D: Appl. Phys. **46** (2013) 255001 (6pp) doi:10.1088/0022-3727/46/25/255001

Magnetic domain studies of $La_{0.7}Sr_{0.3}MnO_3$ film deposited on $SrLaAlO_3$ (0 0 1) substrate

Chi-Ching Liu[1,2,3], Pei-Yuan Chu[1], Yao-Wei Chiang[1], Jenh-Yih Juang[1] and Shien-Uang Jen[2]

[1] Department of Electrophysics, National Chiao Tung University, Hsinchu, Taiwan, Republic of China
[2] Institute of Physics, Academia Sinica, Taipei, Taiwan, Republic of China

E-mail: cloudboy1982@hotmail.com

Received 25 January 2013, in final form 1 May 2013
Published 7 June 2013
Online at stacks.iop.org/JPhysD/46/255001

Abstract
Epitaxial 120 nm $La_{0.7}Sr_{0.3}MnO_3$ (LSMO) compressively strained thin films were deposited on single-crystalline $SrLaAlO_3$(0 0 1) (SLAO) substrates by the pulsed laser deposition (PLD) method. From the x-ray diffraction study, we confirmed that the *c*-axis of the LSMO crystal pointed out of the film plane. Two kinds of magnetic experiments were performed on the film: (i) the in-plane (field $H \equiv H_P$) and the out-of-plane (field $H \equiv H_N$) magnetic hysteresis loop measurements and (ii) magnetic force microscopy scans. We have proved from both theory and experiment that the LSMO film should exhibit the *weak and tilted* perpendicular magnetic anisotropy at room temperature (RT), that is, the easy axis (EA) is tilted relative to the film normal by an angle $\theta_o \fallingdotseq 37^\circ$, when the film is in the demagnetized state. The magnetic domain (MD) structure of the demagnetized LSMO film showed a maze-like pattern. Although from the in-plane hysteresis loop, $H_P = 600$ Oe seems large enough to saturate the film, the corresponding MD structure was not in a single-domain state. Instead, there were two types of MDs: the canted MD and the saturated MD. The MD patterns of the LSMO film between the demagnetized and the remanent states were different. In addition, there were double-switch phenomena in the out-of-plane hysteresis loop. When $|H_N| \cong 140$ Oe, a transition of the MD pattern from the maze-like to the closure (or dense-stripe) type occurred.

(Some figures may appear in colour only in the online journal)

1. Introduction

Perovskite manganites have demonstrated rich emergent physics owing to the strong correlations among the charge, spin, orbital, and lattice degrees of freedoms. One of the unique magnetic and electronic behaviours of perovskite manganites is colossal magnetoresistance (CMR), which has drawn much interest due to the possibility of making magnetic devices that utilize this effect [1]. Some of the perovskite manganites exhibit the ferromagnetic and metallic properties below their Curie temperatures (T_C) and the paramagnetic and insulating properties at a temperature higher than their T_Cs, respectively [2–5]. 'Double exchange' is one of the theoretical models ubiquitously adopted to interpret these interesting properties in these compounds. The theory considers the magnetic coupling between Mn^{3+} and Mn^{4+} ions, which result from the motion of electrons between the two partially filled d shells with strong on-site Hund's coupling [6–9].

In this article, we report that we have deposited the $La_{0.7}Sr_{0.3}MnO_3$ (LSMO) thin films on $SrLaAlO_3$(0 0 1) (SLAO) substrates and, in particular, studied the magnetic domain (MD) properties of the films. Although previous studies [10–12] have already shown the maze-like MD patterns of the LSMO films in various film thicknesses, they did not study the MD patterns at nonzero field. Here, we concentrate on how the MD patterns are changed, as the in-plane (IP) (H_P) and/or out-of-plane (OFP; H_N) magnetic fields are varied.

[3] Author to whom any correspondence should be addressed.

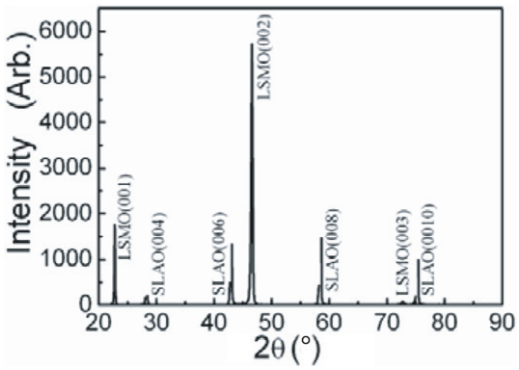

Figure 1. The x-ray diffraction pattern of the LSMO film grown on an SLAO(0 0 1) substrate. The *c*-axis of the LSMO film is perpendicular to the film plane.

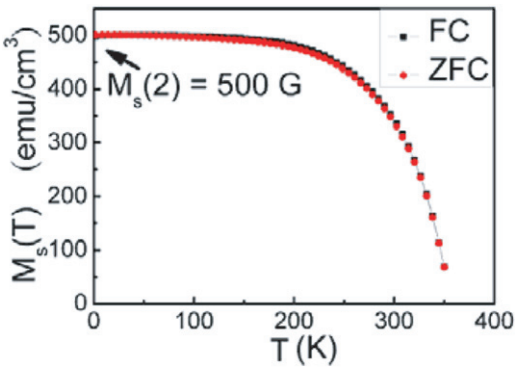

Figure 2. Temperature (T) dependence of saturation magnetization (M_S) of the LSMO film. FC means field cool under an in-plane magnetic field of 1 KOe, and ZFC means zero-field cool.

2. Experimental details

LSMO films with a fixed thickness (t_f) of about 120 nm were deposited on single-crystalline SLAO(0 0 1) substrates, using a 248 nm KrF excimer laser operating at energy of 3 mJ and a repetition rate of 5 Hz. To obtain single-crystalline LSMO films, the substrate temperature (T_S) was kept at 750 °C and the oxygen partial pressure (P_{O_2}) was kept at 0.3 Torr. Immediately after deposition, the film was quenched from 750 to 60 °C. The composition of the LSMO film was analyzed by an SEM-EDS device: La : Sr : Mn : O = 12.4 : 5.4 : 15.5 : 66.7 (in at%).

The temperature dependences of magnetization (M) and magnetotransport properties of the LSMO films were measured using a MPMS-XL superconducting quantum interference device (SQUID) system, and the measurement temperature was varied from 2 to 350 K. Major and minor magnetic hysteresis loops were obtained from vibrating sample magnetometer (VSM) measurements with the OFP field H_N and the IP field H_P, respectively. From the OFP hysteresis loop, we obtained the coercivity (H_C), magnetization (M_S(OFP)) at $H_N = H_m = 6$ KOe, and squareness ratio (SQR $= M_r/M_S$, where M_r is magnetic remanence) at RT. Similarly, from IP hysteresis loop, we obtained M_S(IP) at $H_P = H_m$.

MD images of an LSMO film were obtained using the DI-NanoScope IIIa-D3100 magnetic force microscopy (MFM) system. The tapping tip used was a model PPP-LM-MFR probe. Hard magnetic material coated on the tip gives a coercivity, of approximately 250 Oe, and remanence magnetization, of approximately 150 G. The tip radius of curvature is about 30 nm, and the magnetic resolution is better than 35 nm. The maximum H_P we could apply, associating with our MFM system, was 600 Oe.

The electrical resistance (R) was measured by the standard four-point-probe method. The crystalline structure of the films was examined by x-ray diffraction (XRD) (θ–2θ scan) using $CuK_{\alpha 1}$ line measurements.

3. Results and discussion

The XRD pattern of the LSMO/SLAO(0 0 1) film is shown in figure 1. The high-T_S-grown LSMO film is single crystalline, with the *c*-axis pointing out of the film plane. The LSMO bulk is cubic with $a_B = 3.885$ Å [13], and the SLAO(0 0 1) substrate is tetragonal with $a = b = 3.756$ Å and $c = 12.637$ Å[4]. From the x-ray structure data above, we conclude that the LSMO film is almost matched for the *a*- and *b*-axes in the plane with the SLAO(0 0 1) substrate, that is, the IP lattice mismatch at film/substrate interface is $\Delta\varepsilon = -3.43\%$ (a compressive strain), but in the bulk of the LSMO film, $a_f = b_f = 3.883$ Å and $c_f = 3.899$ Å, and $c_f/a_f = 1.003$ (a very small tetragonality for the LSMO/SLAO film).

Figure 2 shows the temperature (T) dependence M_S under an external IP field $H_E = 1$ KOe for the LSMO film ($t_f = 120$ nm) on SLAO(0 0 1). From this figure, we can easily find the Curie temperature (T_C) of the LSMO film by extrapolation of the $(M_S)^2$ versus T plot toward the $M_S = 0$ axis; the T_C is 350 K. Hence, the LSMO/SLAO(0 0 1) film should remain ferromagnetic at RT (about 300 K). From figure 2, we also find that at $T = 2$ K, $M_S(2) \equiv M_S$(2-Exp) = 500 G, which corresponds to $3.2\mu_B$/Mn. As this value is close to $3.8\mu_B$/Mn, our LSMO film should also show high-quality magnetic and electrical properties [14]. Nevertheless, there are still discrepancies as to why our measured $3.2\mu_B$/Mn is lower than the quoted $3.8\mu_B$/Mn [14] and also our measured $T_C = 350$ K is lower than the quoted $T_C = 370$ K [15]. The explanations will be given later, when we discuss equation (6) and the MD pattern in figure 4(*b*). In short, we believe that the MD pattern for figure 2 was not in a single-domain state, even though from the VSM measurement and under $H_E = 1$ KOe field we seemed to have reached saturation. Apparently, the maximum 1 KOe field used is still not large enough to saturate the film. Thus, the M_S versus T curve in figure 2 should be shifted upward (or corrected) with respect to the data in [15]. In other words, M_S(2-Th) = (3.8/3.2) × 500 = 595 G.

In addition, for later discussion, we would like to estimate M_S at RT. According to the mean field theory (MFT), the thermal-fluctuation effect will make $M_S(2)$ to decrease to M_S, as T increases form 2 K to RT [16]. From figure 4.5 of [16], the theoretical M_S versus T fitting curve (for Ni) based on the MFT predicts that when (RT)/$T_C = 0.81$, M_S/M_S(2-Th) = 0.62. Thus, we may find $M_S = M_S$(2-Th) × 0.62 = 370 G for the LSMO film.

[4] Data sheet issued by the manufacturer, the MTI Corporation.

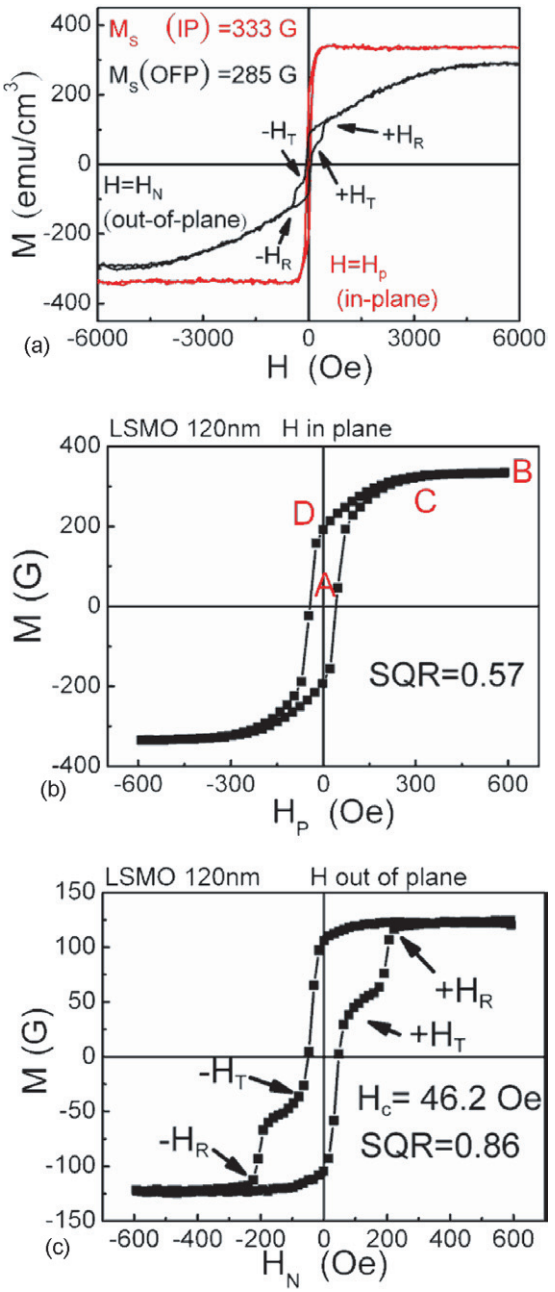

Figure 3. (*a*) The major hysteresis loops with the in-plane (H_P) field (in red) and the out-of-plane (H_N) field (in black). (*b*) The minor hysteresis loop with $H = H_P$. (*c*) The minor hysteresis loop with $H = H_N$. All the hysteresis-loop measurements were made at room temperature (RT).

We also measured R as a function of T from 300 to 15 K. R decreases from 22.7 to 1.7 Ω, as T decreases monotonically. The R versus T plot follows Matthiessen's rule with the residual resistance ratio RRR = 13, which means that the LSMO/SLAO(0 0 1) film is not only ferromagnetic but also metallic at RT. Interesting to notice is that slightly above RT (i.e. around $T = 350\,\mathrm{K} \cong T_C$), there is also a metal–insulator transition [14, 15].

Figure 3(*a*) shows the OFP (H_N) and IP(H_P) major magnetic hysteresis loops of the LSMO film, respectively, with the maximum fields (H_m) being ±6 KOe. Judging from these two figures, we may first think that the EA of the film is lying in the film plane. Also, at $H = H_m$, we easily saturate the film with H_P, but still we cannot saturate the film with H_N. Thus, M_S(IP) = 333 G, which is larger than M_S(OFP) = 285 G at RT. These phenomena are very confusing. It is no wonder in [10] that they reached a controversial conclusion that the perpendicular maze-like MD of the LSMO film is uncorrelated to the directions of EA. In the later discussion, we believe that our LSMO film does show the *weak and tilted* perpendicular anisotropy, which should result in some peculiar (or anomalous) magnetic hysteresis behaviours, and conclude that EA is inclined relative to the film normal by a small angle θ_o. Thus, from the M versus H_P virgin curve (the red line) in figure 3(*a*), we calculate the (experimental) magnetic anisotropy (K_P) of the LSMO film; K_P is about $3.77 \times 10^5\,\mathrm{erg\,cm^{-3}}$. Notice that if EA were completely IP, the anisotropy energy product under the M versus H_N virgin curve would be unrealistically large, for example, of the order of $10^7\,\mathrm{erg\,cm^{-3}}$, even after demagnetization corrections. We have also shown the minor H_P and H_N magnetic hysteresis loops in figures 3(*b*) and (*c*). Up to now, it is also noticed that M_S(IP) = 333 G < M_S = 370 G at RT, which seems contradictory. This apparent inconsistency will be explained later, when we discuss the MD pattern of the LSMO film.

Theoretically speaking, we can calculate the magnetoelastic anisotropy (K_σ) from the following two equations:

$$K_\sigma = -(3/2) S_i \lambda_S (\cos^2 \xi) \tag{1a}$$

$$S_i = E(\Delta\varepsilon)_{ave}, \tag{1b}$$

S_i is the intrinsic IP compressive stress, ξ is the angle between the stress axis and $\overrightarrow{M_S}$, $E = 562$ GPa is Young's modulus [17], $(\Delta\varepsilon)_{ave} = (a_f - a_B)/a_f = -0.05\%$, and $\lambda_S = 200$ ppm is the saturation magnetostriction [18] of the LSMO film. Note that in equations (1*a*) and (1*b*), we have used $(\Delta\varepsilon)_{ave}$, instead of $(\Delta\varepsilon)$, because the strain $(\Delta\varepsilon)$ at the interface is usually largely relaxed over a short distance (about 25 nm) from the interface. Hence, the IP average strain $(\Delta\varepsilon)_{ave}$ in the bulk of the 120 nm film is estimated to be −0.05% [19]. Moreover, because the thermal expansion coefficient of LSMO is almost the same as that of SLAO, the thermal strain on LSMO film is negligible, only +0.01%. By taking $(\Delta\varepsilon)_{ave} = -0.05\%$, K_σ estimated from equations (1*a*) and (1*b*) will not be very large, which is also the reason $\overrightarrow{M_S}$ can be rotated into the film plane with a low H_P, about 300 Oe only, as shown in figure 3(*b*). Next, as $S_i < 0$ and $\lambda_S > 0$, the EA, defined by K_σ, must be normal to the film plane, that is, $\xi = 90°$. In turn, the magnetostatic (or demagnetizing) energy (E_M), which tends to force $\overrightarrow{M_S}$ IP, is expressed as follows:

$$E_M = (1/2) H_d M_S, \tag{2a}$$

$$H_d = N_d(M_S), \tag{2b}$$

where $N_d = 4\pi$ is the demagnetizing factor along the film normal. Thus, from equations (1*a*) and (1*b*), we find $K_\sigma = 8.43 \times 10^5\,\mathrm{erg\,cm^{-3}}$, and from equations (2*a*) and (2*b*), $E_M = 6.56 \times 10^5\,\mathrm{erg\,cm^{-3}}$. The theoretical estimation of $K_\sigma - E_M = 1.87 \times 10^5\,\mathrm{erg\,cm^{-3}}$, which is close to the value of K_P. Moreover, the theoretical (Q_{th}) and experimental

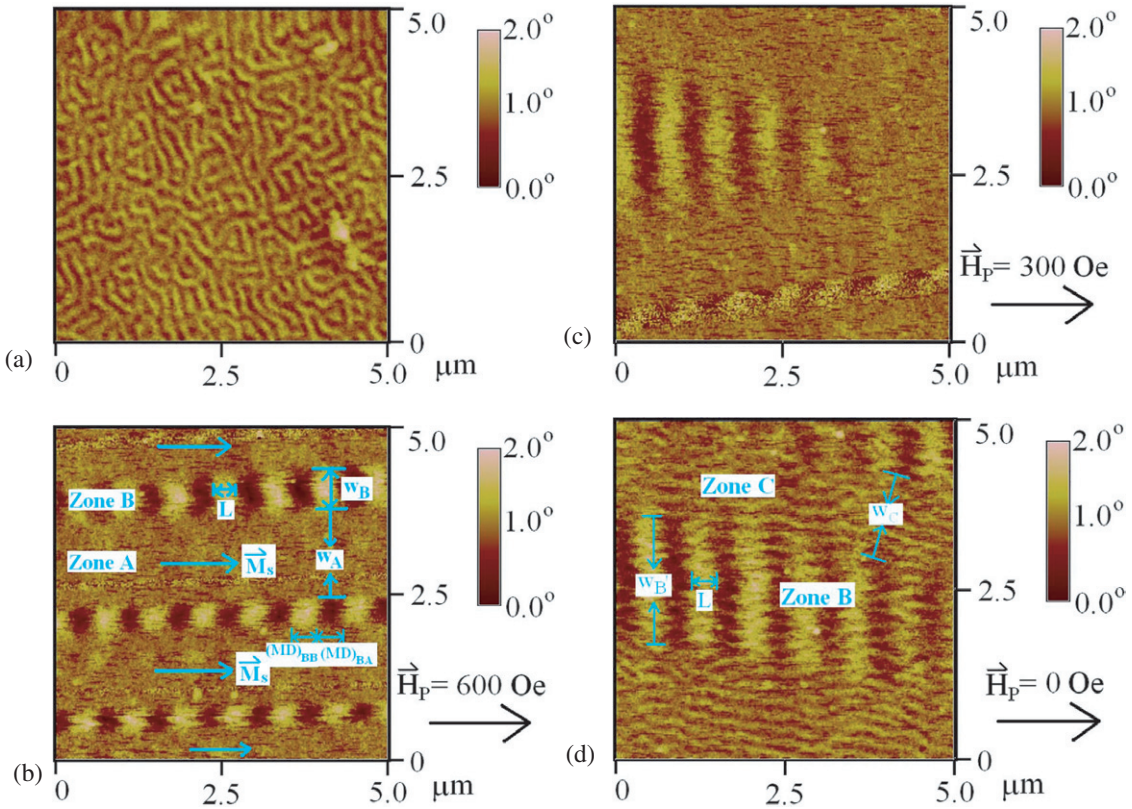

Figure 4. Magnetic domain patterns of the LSMO film under various conditions: (*a*) in a demagnetized state (corresponding to state A in figure 3(*b*)); (*b*) when an in-plane field $H_P = 600$ Oe was applied (to state B); (*c*) when $H_P = 300$ Oe was applied (to state C); and (*d*) when H_P was reduced to zero (to the remanent state or state D).

(Q_{exp}) quality factor can be defined as $Q_{th} \equiv |K_\sigma|/E_M$ and $Q_{exp} \equiv K_P/E_M$, respectively [20]. Simple calculation shows that $Q_{th} = 1.3$ and $Q_{exp} = 0.5$. As $0.4 < Q_{exp}$ or $Q_{th} < 1.5$ for our LSMO film, it should exhibit the *weak and tilted* perpendicular magnetic anisotropy (WTPMA), defined in [21]. In other words, due to the balance of torques, $M_S H_K \sin\theta_o = M_S H_d \cos\theta_o$, where $H_K \equiv |2K_\sigma|/M_S$, the EA in each MD should be tilted from the normal of the film by an angle θ_o, where $\theta_o = \tan^{-1}(H_d/H_K) = \tan^{-1}(1/Q_{th}) = 37^\circ$. Moreover, figures 3.121–3.123 and 5.89 in [21] have shown that in this kind of WTPMA film, the MD pattern can be either the maze-like or the WTPMA-closure (i.e. the dense-stripe) type. A good example is that for a thick permalloy film (210 nm), they have observed the dense-stripe MDs and the anomalous magnetic hysteresis curve, as figure 5.91 in [21], which is similar to the M versus H_N plot in figure 3(*a*). Notice that there is a clear distinction between the conventional-stripe and the dense-stripe MDs by our definitions. In the former case, EA is IP and the size (or width) of MD (or stripe) is usually quite large, about 10–100 μm, whereas in the latter case, EA is OFP and the MD size is small, only about 0.1–1.0 μm.

Figure 4(*a*) shows an MFM image, taken in a zero field and at RT of the LSMO films in a completely demagnetized state. The scanning size was typically 5 μm × 5 μm. The observed bright and dark contrast images represent the up and down MDs, respectively, with the perpendicular anisotropy. The MD width (d) is about 0.1 μm. This MFM image is the classical maze-like MD pattern, which represents the MD structure at state A (i.e. the demagnetized state at $H_P = 0$ Oe) in figure 3(*b*). Figure 5(*a*) shows the cross-sectional view of the maze-like MDs in figure 4(*a*). As mentioned before, $\overrightarrow{M_S}$ or EA of the LSMO film (figure 5(*a*)) is tilted from the c-axis by an angle $\theta_o = 37^\circ$. From [16, 22], MD width (d) is written as follows:

$$d = \sqrt{\frac{\sigma_{exp} t_f}{1.70(M_S \cos\theta_o)^2}}, \tag{3}$$

where σ_{exp} is the (experimental) domain wall (MDW) energy per unit area, t_f is the film thickness, and M_S is the saturation magnetization in each MD. By taking the following data, $d = 0.1\,\mu$m, $t_f = 120$ nm and $M_S \approx 370$ emu cm^{-3} into equation (3), we find that $\sigma_{exp} \approx 0.93$ erg cm^{-2} for our LSMO film. Moreover, we would like to compare σ_{exp} and σ_{th}. From [21], the (theoretical) MDW energy (σ_{th}) of a 180° Bloch wall is expressed as follows:

$$\sigma_{th} = 4\sqrt{AK_P}, \tag{4a}$$

$$A = [J_{ex} S^2]/a, \tag{4b}$$

where A is the MDW stiffness, $J_{ex} = 2.4 \times 10^{-15}$ erg is the exchange integral [23], and $S = 1.85$ is the spin number [23] of the LSMO film. Based on equations (4*a*) and (4*b*), a simple calculation shows that $\sigma_{th} = 1.13$ erg cm^{-2}.

Figure 4(*b*) shows the MFM image of the LSMO film under an IP (or HA) field $H_P = 600$ Oe. This image shows the MD structure at state B in figure 3(*b*). Although at state B, we seem to have saturated the LSMO film in the

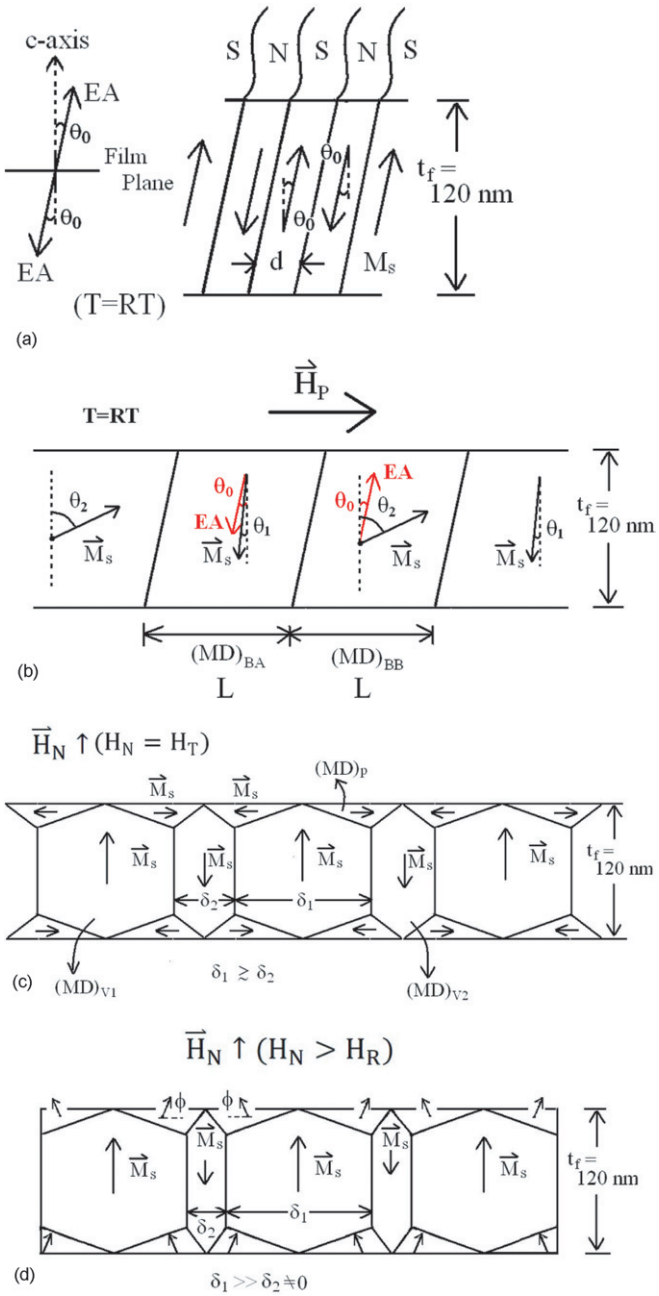

Figure 5. (*a*) The cross-sectional view of the maze-like magnetic domains (MDs) of figure 4(*a*). θ_o is the tilting angle between EA and the *c*-axis. (*b*) The cross-sectional view of the MDs in zone B of figure 4(*b*): saturation magnetization, $\overrightarrow{M_S}$, in $(MD)_{BA}$ or $(MD)_{BB}$, is canted with an angle θ_1 or θ_2 by an in-plane field H_P. (*c*) The proposed closure (or dense-stripe) MD structure when $H_N = H_T$, which is defined in figure 3(*b*). δ_1 and δ_2 are MD widths of $(MD)_{V1}$ and $(MD)_{V2}$, respectively. (*d*) The proposed closure (or dense-stripe) MD structure when $H_N > H_R$, which is defined in figure 3(*b*).

hard direction (both for the major and minor loops), the MD structure of figure 4(*b*) does not exhibit the single-domain structure. Instead, in figure 4(*b*), we find two kinds of MDs: one is defined as the saturated MD in zone A and the other as the canted MD in zone B. The reason for this complicated MD formation is unclear to us. As shown in figure 4(*b*), $\overrightarrow{M_S}$ of the MD in zone A lies in the film plane and points along the same direction as $\overrightarrow{H_P}$. The width (w_A) of the MD in zone A ranges from 1.11 to 1.40 μm. The cross-sectional view of the MD in zone B is schematically shown in figure 5(*b*), where due to the K_P and Zeeman effect of H_P, $\overrightarrow{M_S}$ in domain $(MD)_{BA}$ is rotated from the *c*-axis by an angle θ_1 and $\overrightarrow{M_S}$ in domain $(MD)_{BB}$ by an angle θ_2. Theoretically, the total energy (E_A) of $(MD)_{BA}$ and that (E_B) of $(MD)_{BB}$ are expresses as follows:

$$E_A = K_P \sin^2(\theta_o - \theta_1) + M_S H_P \sin(\theta_1), \qquad (5a)$$

$$E_B = K_P \sin^2(\theta_2 - \theta_o) - M_S H_P \sin(\theta_2). \qquad (5b)$$

Under the conditions, $d(E_A)/d\theta_1 = 0$ and $d(E_B)/d\theta_2 = 0$, equations (5*a*) and (5*b*) can be solved graphically for θ_1 and θ_2 with the known parameters θ_o and $\eta = (M_S H_P)/(2K_P)$. Hence, when $H_P = 600$ Oe, we could find $\theta_1 = 29^\circ$ and $\theta_2 = 49^\circ$.

As $\theta_1 \neq 90^\circ$ and $\theta_2 \neq 90^\circ$, the (longitudinal) magnetization in zone B is not pulled all the way along the field direction. Furthermore, the width (w_B) of the MD in zone B ranges from 0.39 to 0.45 μm, and the length (L) of $(MD)_{BA}$ is the same as that of $(MD)_{BB}$, about 0.37 μm. Thus, based on the MD structures of figures 4(*b*) and 5(*b*), the expected (or predicted) M at the state B should be written as follows:

$$M(@\text{ state B}) = M_S\left[\frac{w_A}{w}\right] + \left(\frac{1}{2}\right) M_S\left[\frac{w_B}{w}\right][\sin\theta_2 - \sin\theta_1], \qquad (6)$$

where $w = w_A + w_B$. By substituting into equation (6) with the values of $M_S = 370$ G, w_A, w_B, θ_1 and θ_2, we obtain M(@ state B) = 299 G, which is close to the experimental M_S(IP) = 333 G, from figures 3(*a*) and (*b*), when H_P is either equal to 600 Oe or 6 KOe. Here, at least, we explained why M_S should be larger M_S(IP) or M(@ state B).

Next, figure4(*c*) shows the MFM image of the LSMO films, when $H_P = 300$ Oe, which corresponds to state C in figure 3(*b*). Figure 4(*d*) shows the MFM image of the LSMO film, when H_P is reduced to zero, which corresponds to the remanent state (or state D) in figure 3(*b*). There are also two kinds of MDs in figure 4(*d*): the MD in zone B and the MD in zone C. Comparing figures 4(*b*), (*d*) and 5(*b*), we could summarize the following four findings. First, w_B' of the MD in zone B has grown wider, about 1.88 μm, as H_P is decreased from 600 to 0 Oe. Second, as to the MDs in zone C of figure 4(*d*), they are just the dense-stripe MDs, with tilted $\overrightarrow{M_S}$, like those shown in figure 4(*a*) or 5(*a*). A small difference between the MD structures at the demagnetized state in figure 4(*a*) and that in zone C at the remanent state in figure 4(*d*) is that the former is in a maze-like pattern, whereas the latter is in a dense-stripe pattern and the MD walls (MDWs) in zone C are nearly parallel (∥) to the direction of H_P, that is, a partial reorientation effect of MDW only in zone C by H_P. However, it is also interesting to note that the MDWs in zone B in figure 4(*d*) remain perpendicular (⊥) to the direction of H_P. Although [24] has made some calculations based on the magnetostrictive mechanism, the relevant explanation for the influences on different types (∥ and ⊥) of MDWs by H_P, as disclosed above, is far from complete. Third, L of $(MD)_{BA}$ or $(MD)_{BB}$ in zone B remains the same, as H_P decreases. Fourth, θ_1 in $(MD)_{BA}$ or θ_2 in $(MD)_{BB}$ should be relaxed to a value

close to, but not equal to, θ_o, as H_P decreases to zero. This also agrees with the fact that SQR at the remanent state (or state D) is not zero. $\theta_o \neq 0^\circ$ at the remanent state also indicates that due to the WTPMA, the IP magnetization can still exist in some areas (or parts) in the LSMO film. Because of the hysteresis effect, at $H_P = 0$ Oe, there should be two magnetization states, the demagnetized (A) and the remanent (D) states, which are associated with different MD patterns, as shown in figures 4(*a*) and (*d*), respectively.

Because we could not apply H_N in our MFM system, the following arguments are based on a theoretical model from [21]. In figure 3(*c*), the M versus H_N hysteresis loop shows the two-step (or double) switching phenomena. As we found $0.4 < Q < 1.5$ for our LSMO film, according to [21], the closure (or dense-stripe) MD structure is completely feasible at $H_N \neq 0$ Oe. Thus, we believe that when $0 < H_N < H_T \cong 140$ Oe, there is an MDW motion, which causes the first Barkhausen jump in M; when $H_N = H_T$, there is a transition of the MD pattern from figure 5(*a*), the maze-like pattern, to figure 5(*c*), the closure pattern; when $H_T < H_N < H_R \cong 240$ Oe, there is an MDW motion again, causing the second jump; and finally, when $H_N > H_R$, there are slow (or gradual) rotations of magnetization. In figure 5(*c*), where $H_N = H_T$, we have the following features. First, the $\overrightarrow{M_S}$ in the columnar MDs, $(MD)_{V1}$ and $(MD)_{V2}$, is perpendicular, and the $\overrightarrow{M_S}$ in the triangular $(MD)_{PS}$ is IP. Second, the width (δ_1) of $(MD)_{V1}$ is slightly larger than that (δ_2) of $(MD)_{V2}$, when $H_N = H_T$. In figure 5(*d*), where $H_N > H_R$, we have $\delta_1 \gg \delta_2$, and in the triangular $(MD)_{PS}$, each $\overrightarrow{M_S}$ starts to rotate toward the perpendicular direction. Because the *local* demagnetizing field near the surface and/or the interface regions is extremely large, it is rather difficult to turn $\overrightarrow{M_S}$ in the triangular $(MD)_P$ from IP to OFP, that is, ϕ can only increase very slowly with increasing H_N. This explains why in the range $H_N > H_R$ in figure 3(*a*), the magnetization (M) increases gradually, and even when $H_N = 6$ KOe, the film is still not saturated.

4. Summary

We have made $t_f = 120$ nm LSMO single-crystal films on SLAO substrates at $T_S = 750\,^\circ$C by the pulsed laser deposition method. The LSMO film is metallic and ferromagnetic below 350 K. OFP and IP magnetic hysteresis loops and the MFM measurements were performed on the LSMO/SLAO(0 0 1) films, respectively. We found that (I) the magnetic moment of the LSMO/SLAO film at $T = 2$ K is $3.2\mu_B$/Mn; (II) from the theoretical calculation, the LSMO film exhibits the *weak and tilted* perpendicular anisotropy with EA inclined at an angle $\theta_o = 37^\circ$ relative to the normal of the film plane; (III) H_C is about 46.2 Oe; (IV) the MD structure of the demagnetized LSMO film is in a maze-like pattern; (V) the MDW energy σ_{exp} of the LSMO film is 0.93 erg cm^{-2}; (VI) although from the IP hysteresis loop, $H_P = 600$ Oe seems large enough to saturate the film, the corresponding MD structure is not in a single-domain state; (VII) the MD patterns of the LSMO film between the demagnetized and the remanent states are different; and (VIII) a decreasing H_P tends to reorient the MDWs parallel to H_P only in zone C, but MDWs in zone B remain perpendicular to H_P.

Acknowledgments

SUJ is grateful to National Science Council for the financial support from grant no NSC-100-2112-M001-017-MY03-(2/3). JYJ is supported by grant no NSC-101-2112-M-009-015-MY2 and partially by the MOE-ATU programme operated at NCTU.

References

[1] Schiffer P, Ramirez A P, Bao W and Cheong S W 1995 *Phys. Rev. Lett.* **75** 3336
[2] Laverdiere J, Jandl S and Fournier P 2011 *Phys. Rev.* B **84** 104434
[3] Salamon M and Jaime M 2001 *Rev. Mod. Phys.* **73** 583
[4] Dho J, Kim W S and Hur K H 2002 *Phys. Rev. Lett.* **89** 027202
[5] Cheng T Y *et al* 2006 *Phys. Rev.* B **74** 134428
[6] Zener C 1951 *Phys. Rev.* **82** 403
[7] Anderson P W and Hasegawa H 1955 *Phys. Rev.* **100** 675
[8] de Gennes P G 1960 *Phys. Rev.* **118** 141
[9] Hwang H Y, Cheong S W, Ong N P and Batlogg B 1996 *Phys. Rev. Lett.* **77** 2041
[10] Bakaul S R, Lin W and Wu T 2011 *Appl. Phys. Lett.* **99** 042503
[11] Dho J, Kim Y N, Hwang Y S, Kim J C and Hur N H 2003 *Appl. Phys. Lett.* **82** 1434
[12] Houwman E P, Maris G, De Luca G M, Niermann N, Rijnders G, Blank D H A and Speller S 2008 *Phys. Rev.* B **77** 184412
[13] Abrutis A, Plausinaitiene V, Kubilius V, Teiserskis A, Saltyte Z, Butkute R and Senateur J P 2002 *Thin Solid Films* **413** 32
[14] Boschker H *et al* 2011 *J. Phys. D: Appl. Phys.* **44** 205001
[15] Urushibara A, Moritomo Y, Arima T, Asamitsu A, Kido G and Tokura Y 1995 *Phys. Rev.* B **51** 14103
[16] Chikazumi S1978 *Physics of Magnetism* (New York: Krieger)
[17] Huang Q J, Cheng Y, Liu X J, Xu X D and Zhang S Y 2006 *Ultrasonics* **44** e1223
[18] Dabrowski B, Gladczuk L, Wisniewski A, Bukowski Z and Dybzinski R 2000 *J. Appl. Phys.* **87** 3011
[19] Zhai Z Y, Wu X S, Jiang Z S, Hao J H, Gao J, Cai Y F and Pan Y G 2006 *J. Appl. Phys.* **89** 262902
[20] Malozemoff A P and Slonczewski J C 1979 *Magnetic Domain Walls in Bubble Materials* (New York: Academic)
[21] Hubert A and Schäfer R 2000 *Magnetic Domains* (Berlin: Springer)
[22] Cullity B D 1972 *Introduction to Magnetic Materials* (Reading, MA: Addison-Wesley)
[23] Boschker H, Kautz J, Houwman E P, Koster G, Blank D H A and Rijnders G 2010 *J. Appl. Phys.* **108** 103906
[24] Patterson R W and Muller M W 1972 *Int. J. Magn.* **3** 293